

# Mechanism of Photosensitized Generation of Singlet Oxygen during Oxygen Quenching of Triplet States and the General Dependence of the Rate Constants and Efficiencies of $O_2(^1\Sigma_g^+)$ , $O_2(^1\Delta_g)$ , and $O_2(^3\Sigma_g^-)$ Formation on Sensitizer Triplet State Energy and Oxidation Potential

Claude Schweitzer,<sup>†</sup> Zahra Mehrdad, Astrid Noll, Erich-Walter Grabner, and Reinhard Schmidt\*

*Institut für Physikalische und Theoretische Chemie, Johann Wolfgang Goethe-Universität, Marie-Curie-Strasse 11, D60439 Frankfurt am Main, Germany*

*Received: May 27, 2002; In Final Form: November 13, 2002*

Rate constants of photosensitized generation of  $O_2(^1\Sigma_g^+)$ ,  $O_2(^1\Delta_g)$ , and  $O_2(^3\Sigma_g^-)$  have been determined for a series of  $\pi\pi^*$  triplet sensitizers with strongly varying oxidation potential ( $E_{ox}$ ), triplet energy ( $E_T$ ), and molecular structure, in  $CCl_4$ . We demonstrate that one common dependence on  $E_{ox}$  and  $E_T$  successfully describes these rate constants for the molecules studied here and also for all previously investigated  $\pi\pi^*$  sensitizers, independently of molecular structure or any other parameter. Photosensitized singlet oxygen generation during  $O_2$  quenching of  $\pi\pi^*$  triplet states can be generally described by a mechanism involving the successive formation of excited noncharge transfer (nCT) encounter complexes and partial charge transfer (pCT) exciplexes of singlet and triplet multiplicity  $^{1,3}(T_1^3\Sigma)$ , following interaction of  $O_2(^3\Sigma_g^-)$  with the triplet excited sensitizer. Both  $^{1,3}(T_1^3\Sigma)$  nCT and pCT complexes decay by internal conversion (ic) to yield  $O_2(^1\Sigma_g^+)$ ,  $O_2(^1\Delta_g)$ , and  $O_2(^3\Sigma_g^-)$  and the sensitizer ground state. ic is the rate-limiting step in the nCT channel, whereas exciplex formation is rate determining in the pCT channel. Rotation of the  $O_2$  molecule within the solvent cage of  $^{1,3}(T_1^3\Sigma)$  nCT complexes is fast enough to allow for a completely established intersystem crossing (isc) equilibrium, whereas significant noncovalent binding interactions slow rotation and inhibit isc between  $^1(T_1^3\Sigma)$  and  $^3(T_1^3\Sigma)$  pCT complexes. Upon the basis of this mechanism, we propose a semiempirical relationship that can be generally used to estimate rate constants and efficiencies of photosensitized singlet oxygen generation during  $O_2$  quenching of  $\pi\pi^*$  triplet states in  $CCl_4$ . The data set includes 127 rate constants for derivatives of naphthalene, biphenyl, fluorene, several ketones, fullerenes, porphyrins and metalloporphyrins, and other homocyclic and heterocyclic aromatics of variable molecular structure and size. It is suggested that the general relationship presented here can be used for the optimization of the singlet oxygen photosensitization ability of many molecules, including those used in biological and medical applications, such as the photodynamic therapy of cancer.

## Introduction

The photosensitized production of the lowest excited singlet states  $^1\Sigma_g^+$  and  $^1\Delta_g$  of  $O_2$  during oxygen quenching of excited triplet ( $T_1$ ) states is a process of major importance to the chemical, biological, and medical sciences. The first excited state,  $O_2(^1\Delta_g)$ , which is commonly being referred to as singlet oxygen, is an extremely reactive and highly cytotoxic species and is responsible for natural photodegradation processes and photocarcinogenesis, but also has significant applications, for example in organic synthesis and in the photodynamic therapy of cancer. In solution, the second excited singlet state,  $O_2(^1\Sigma_g^+)$ , which can be formed in competition to  $O_2(^1\Delta_g)$ , is very rapidly and quantitatively deactivated to the long-lived  $O_2(^1\Delta_g)$  species.<sup>1,2</sup> Since the pioneering work of Gijzeman et al.,<sup>3</sup> mechanistic studies have endeavored to establish a relationship between the physical properties of a sensitizer and the rate constants and efficiencies of singlet oxygen formation during  $O_2$  quenching

of  $T_1$  states. Significant advances have been made on the basis of correlations with the sensitizer triplet energy  $E_T$  and oxidation potential  $E_{ox}$ , but despite sustained efforts carried out over the past 30 years and a huge amount of experimental data available,<sup>4,5</sup> a general quantitative relationship is still lacking. We will propose here, for the first time, a general relationship that describes how variations of  $E_T$  and  $E_{ox}$  influence the rate constants of formation of  $O_2(^1\Sigma_g^+)$ ,  $O_2(^1\Delta_g)$ , and ground-state oxygen  $O_2(^3\Sigma_g^-)$  during  $O_2$  quenching of  $T_1$  states in  $CCl_4$ .

This relationship relies upon the photosensitization mechanism displayed in Figure 1, which is based on a scheme originally proposed by Gijzeman et al.,<sup>3</sup> and later modified by Wilkinson and co-workers<sup>6–15</sup> and ourselves.<sup>16–18</sup> Figure 1 also features a graphical representation of the conclusions from recent discussions of the structure of intermediate complexes involved in the photosensitized generation of singlet oxygen.<sup>18–21</sup>

The scheme in Figure 1 infers that  $T_1$ -excited sensitizer and  $O_2(^3\Sigma_g^-)$  form, with diffusion-controlled rate constant  $k_{diff}$  ( $2.7 \times 10^{10} \text{ M}^{-1} \text{ s}^{-1}$  in  $CCl_4$ ) excited  $^m(T_1^3\Sigma)$  encounter complexes with multiplicities  $m = 1, 3$  and  $5$ , which either dissociate again with rate constant  $k_{-diff}$  (assumed to be  $k_{-diff} = k_{diff}/M^{-1} = 2.7 \times 10^{10} \text{ s}^{-1}$ , as previously done by Gijzeman et al.,<sup>3</sup> Wilkinson

\* To whom correspondence should be addressed. E-mail: R.Schmidt@chemie.uni-frankfurt.de.

<sup>†</sup> Present address: Department of Chemistry, University of Ottawa, Ottawa, Ontario, Canada.

**"nCT" Encounter Complex**

$O_2$  molecule free to rotate within solvent cage of complex

multiplicity (1, 3, or 5) determined statistically by transient spin configuration, as a consequence of transient geometric position of molecules with respect to each other

several changes of multiplicity may occur within lifetime of nCT complex

**"pCT" Charge Transfer Complex**

restricted mobility of  $O_2$  molecule due to noncovalent binding to sensitizer

multiplicity (1 or 3) determined by multiplicity of precursor encounter complex

no intersystem crossing during pCT complex lifetime

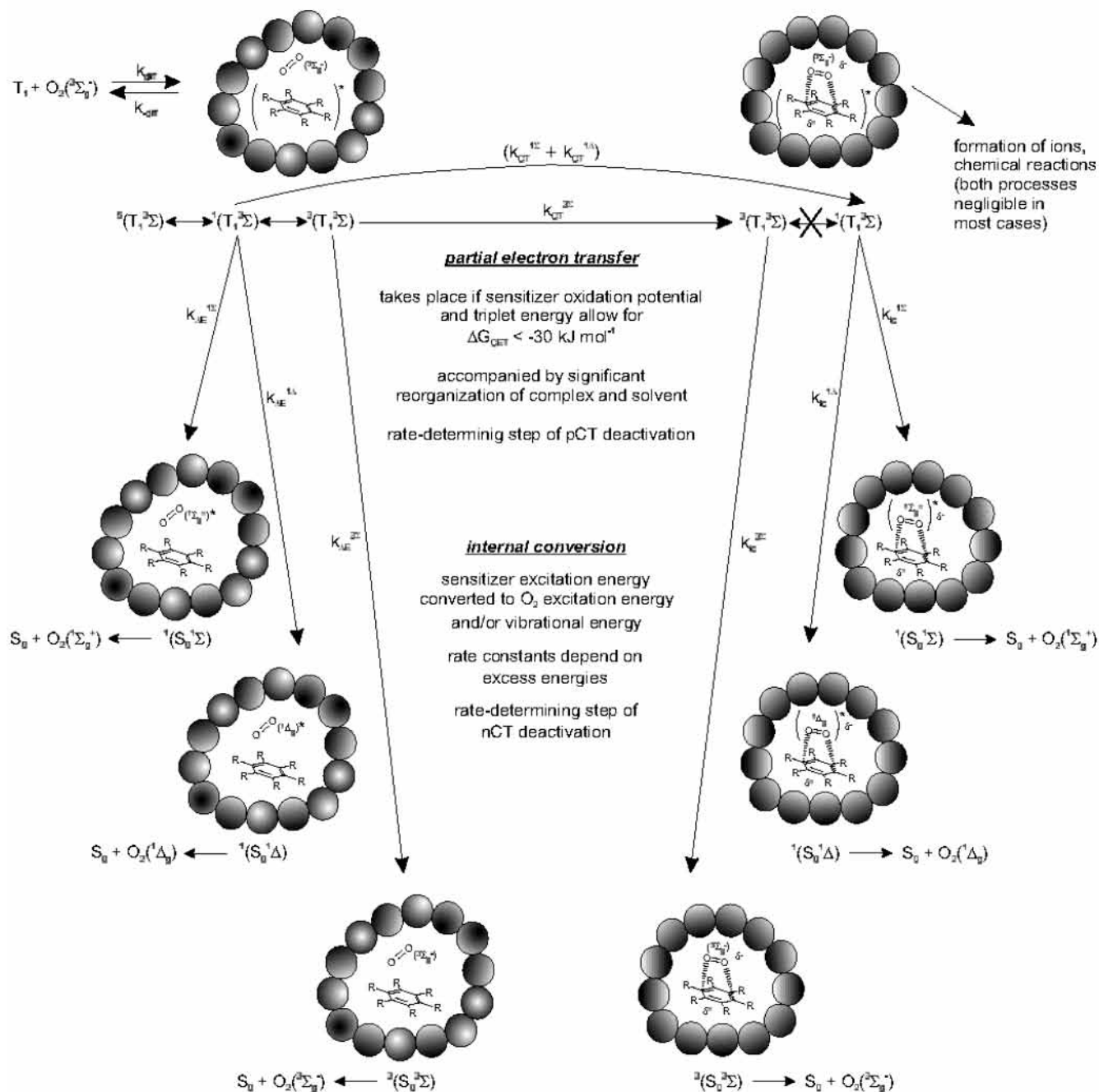


**Figure 1.** Mechanism of photosensitized generation of  $O_2(^1\Sigma_g^+)$ ,  $O_2(^1\Delta_g)$ , and  $O_2(^3\Sigma_g^-)$  during  $O_2$  quenching of triplet states. The scheme shows the different noncharge transfer and partial charge transfer complexes in their solvent cage. The mechanism applies generally to  $\pi\pi^*$  excited aromatic hydrocarbons, including five- and six-membered rings, with and without heteroatoms or metal centers, as we demonstrate here.

et al.,<sup>6-15</sup> and ourselves)<sup>16-21</sup> or yield the quenching products with overall rate constant  $k_D$

$$k_D = k_{-diff}k_T^Q / (k_{diff} - k_T^Q) \quad (1)$$

where  $k_T^Q$  is the experimental quenching rate constant.  $k_D = k_{\Delta E}^{1\Sigma} + k_{\Delta E}^{1\Delta} + k_{\Delta E}^{3\Sigma} + k_{CT}^{1\Sigma} + k_{CT}^{1\Delta} + k_{CT}^{3\Sigma}$  accounts for

the internal conversion (ic) of excited  $^1,3(T_1^3\Sigma)$  encounter complexes with no charge-transfer character (nCT) to the lower-lying nCT complexes  $^1(S_0^1\Sigma)$ ,  $^1(S_0^1\Delta)$ , and  $^3(S_0^3\Sigma)$  (which occurs with rate constants  $k_{\Delta E}^{1\Sigma}$ ,  $k_{\Delta E}^{1\Delta}$ , and  $k_{\Delta E}^{3\Sigma}$ , respectively), as well as for the formation of  $^1(T_1^3\Sigma)$  and  $^3(T_1^3\Sigma)$  partial charge transfer (pCT) complexes, which originates from  $^1,3(T_1^3\Sigma)$  nCT complexes, with rate constants  $(k_{CT}^{1\Sigma} + k_{CT}^{1\Delta})$  and  $k_{CT}^{3\Sigma}$ , respec-

tively. Excited pCT complexes decay by rapid ic ( $k_{ic}^{1\Sigma}$ ,  $k_{ic}^{1\Delta}$ , or  $k_{ic}^{3\Sigma}$ ) to lower-lying pCT complexes, and all species involving the sensitizer ground state ( $S_0$ ) dissociate to give  $S_0$  and  $O_2$ -( $^1\Sigma_g^+$ ),  $O_2$ ( $^1\Delta_g$ ), or  $O_2$ ( $^3\Sigma_g^-$ ).

In the original work of Gijzeman et al.,<sup>3</sup> experimental  $O_2$  quenching rate constants for a series of sensitizers in several solvents were found to be generally smaller than  $1/9k_{diff}$  and to correlate with the sensitizer triplet energy. On the basis of these results, it was suggested that  $O_2$  quenching of excited triplets exclusively proceeds via singlet encounter complexes, and that no isc takes place between the complexes of different multiplicity. However, later studies provided clear evidence for  $k_T^Q$  values in excess of  $1/9k_{diff}$ <sup>6,17,22–28</sup> and even of  $4/9k_{diff}$ ,<sup>29–31</sup> thus showing that complexes of singlet, triplet, and quintet multiplicity can significantly contribute to the overall mechanism. Moreover, a large number of studies showed that, for easily oxidizable molecules, rate constants correlate with the ease of oxidation of the sensitizer, which means that  $O_2$  quenching of  $T_1$  states proceeds, at least partially, via exciplexes.<sup>7–21,23,31,32</sup> However, the dependence of experimental data on redox properties was found to be significantly weaker than expected for a complete electron transfer, and all authors largely agreed that only a partial transfer of charge takes place. Different estimates have been proposed for the charge-transfer character ( $\delta$ ) of the involved exciplexes. For example, a linear interpretation of experimental data for a series of biphenyl derivatives yielded a decrease of  $\delta$  with increasing solvent polarity, from 17% in cyclohexane to 12.5% in acetonitrile,<sup>12</sup> whereas a parabolic Marcus-type model led significantly larger values, and to an increase of  $\delta$  with increasing solvent polarity, from 43% in  $CCl_4$  to 58% in acetonitrile, for the same molecules.<sup>20</sup> In addition to quenching rate constants, a significant number of studies have also provided data on the efficiency  $S_\Delta$  of singlet oxygen formation during  $O_2$  quenching of  $T_1$ , which represents the sum of the efficiencies  $a$  of formation of  $O_2$ ( $^1\Sigma_g^+$ ) and  $b = S_\Delta - a$  of directly formed  $O_2$ ( $^1\Delta_g$ ).<sup>7–21,28,31,32</sup> This allows the calculation of the overall rate constants for  $T_1$  deactivation via the triplet channel,  $k_T^{3\Sigma}$ , and via the singlet channel, ( $k_T^{1\Sigma} + k_T^{1\Delta}$ ), where  $k_T^{1\Sigma}$  and  $k_T^{1\Delta}$  are the rate constants of  $O_2$ ( $^1\Sigma_g^+$ ) and  $O_2$ ( $^1\Delta_g$ ) formation, respectively. Both  $k_T^{3\Sigma}$  and ( $k_T^{1\Sigma} + k_T^{1\Delta}$ ) correlate with sensitizer  $E_{ox}$ , but the dependence was found to be weaker for ( $k_T^{1\Sigma} + k_T^{1\Delta}$ ) in most cases. It was thus concluded that at least the formation of  $O_2$ ( $^1\Delta_g$ ) can occur from both encounter complexes and charge-transfer complexes.<sup>12–15,31,32</sup>

The recent development of novel spectroscopic methods for the time-resolved observation of  $O_2$ ( $^1\Sigma_g^+$ ) allowed us to determine  $a$  and  $b = (S_\Delta - a)$  with sufficient accuracy and, thus, to separate  $k_D$  into the single rate constants of  $O_2$ ( $^1\Sigma_g^+$ ),  $O_2$ ( $^1\Delta_g$ ), and  $O_2$ ( $^3\Sigma_g^-$ ) formation, which are given by eqs 2–4:<sup>1,33</sup>

$$k_T^{1\Sigma} = ak_D \quad (2)$$

$$k_T^{1\Delta} = (S_\Delta - a)k_D \quad (3)$$

$$k_T^{3\Sigma} = (1 - S_\Delta)k_D \quad (4)$$

The first investigation with this technique showed that, for a series of sensitizers with strongly varying  $E_T$ , the multiplicity-normalized rate constants  $k_T^P/m$  (i.e.,  $k_T^{1\Sigma}/1$ ,  $k_T^{1\Delta}/1$ , and  $k_T^{3\Sigma}/3$ ) depend on the excess energy  $\Delta E$  for formation of  $O_2$ ( $^1\Sigma_g^+$ ),  $O_2$ ( $^1\Delta_g$ ), and  $O_2$ ( $^3\Sigma_g^-$ ) from  $^1,3(T_1^3\Sigma)$  encounter complexes, which is given by  $E_T - 157$ ,  $E_T - 94$ , and  $E_T$ , respectively (in  $\text{kJ mol}^{-1}$ ).<sup>34</sup> This is in agreement with the results of Gijzeman

et al.,<sup>3</sup> and also with the early theoretical study of Kawaoka et al.,<sup>35</sup> where the rate constants for the ic from excited  $^1,3,5(T_1^3\Sigma)$  complexes to the lower-lying nCT complexes  $^1(S_0^1\Sigma)$ ,  $^1(S_0^1\Delta)$ , and  $^3(S_0^3\Sigma)$  (represented by  $k_{ic}$  in eq 5) were expressed as a function of the electronic coupling matrix element between initial and final states,  $\beta$ , and of the Franck–Condon factors  $F(\Delta E)$  and the density of final states,  $\rho(\Delta E)$  which both depend on  $\Delta E$

$$k_{ic} = (4\pi^2/h) \rho(\Delta E) F(\Delta E) \beta^2 \quad (5)$$

However,  $k_T^P/m$  data for sensitizers with low oxidation potentials deviate significantly from this correlation, and it was found that, in this case, the  $E_{ox}$  dependence of multiplicity-normalized rate constants for formation of all three  $O_2$  product states becomes more important than the correlation with  $\Delta E$ .<sup>16–18</sup> It was thus suggested that, in general, the multiplicity-normalized rate constants for formation of each  $O_2$  product state are additively composed of a nCT component  $k_{\Delta E}^P/m$  and a pCT component  $k_{CT}^P/m$  (eqs 6–8), which means that formation of  $O_2$ ( $^1\Sigma_g^+$ ),  $O_2$ ( $^1\Delta_g$ ), and  $O_2$ ( $^3\Sigma_g^-$ ) proceeds via both encounter complexes and exciplexes (Figure 1)<sup>16–18</sup>

$$k_T^{1\Sigma}/1 = k_{CT}^{1\Sigma}/1 + k_{\Delta E}^{1\Sigma}/1 \quad (6)$$

$$k_T^{1\Delta}/1 = k_{CT}^{1\Delta}/1 + k_{\Delta E}^{1\Delta}/1 \quad (7)$$

$$k_T^{3\Sigma}/3 = k_{CT}^{3\Sigma}/3 + k_{\Delta E}^{3\Sigma}/3 \quad (8)$$

The study of a series of sensitizers with strongly varying  $E_T$  suggested that the rate constants for the nCT pathway are described by the empirical polynomial of eq 9<sup>34</sup>

$$\log(k_{\Delta E}^P/m) = 9.05 + 9 \times 10^{-3} \Delta E - 1.15 \times 10^{-4} \Delta E^2 + 1.15 \times 10^{-7} \Delta E^3 + 9.1 \times 10^{-11} \Delta E^4 \quad (9)$$

This assumption was also supported by later  $E_{ox}$ -dependent studies, which revealed that the  $k_T^P/m$  values for sensitizers with the highest oxidation potentials, i.e., where CT effects are unlikely, are also described by eq 9.<sup>16–18</sup> Hence, it seems to be established that eq 9 reflects the  $\Delta E$ -dependence of the internal conversion of encounter complexes  $^1,3(T_1^3\Sigma)$  without CT stabilization. However, this dependence is weaker than predicted by eq 5 using  $F'(\Delta E) = \rho(\Delta E)F(\Delta E)$  calculated according to a relationship established by Siebrand<sup>36–38</sup> for the ic between deep potential minima of strongly bound aromatic molecules.<sup>34</sup> It is thus suggested that nCT  $^1,3,5(T_1^3\Sigma)$  complexes involve weak binding interactions and shallow potential minima.<sup>34</sup> Finally, the common  $\Delta E$  dependence of all  $\log(k_{\Delta E}^P/m)$  data also implies that the matrix elements for ic of all  $^1,3(T_1^3\Sigma)$  complexes are the same and that there is a fully established isc equilibrium between nCT encounter complexes.<sup>34</sup>

Using eqs 6–9 to estimate the nCT and pCT contributions to  $k_T^P/m$ , investigations of several series of sensitizers with strongly varying  $E_{ox}$  and constant  $E_T$ <sup>16–18</sup> showed that  $k_{CT}^P/m$  depends on the free energy  $\Delta G_{CET}$  for complete electron transfer from the  $T_1$ -excited sensitizer to  $O_2$ , which is given by the Rehm–Weller equation<sup>39,40</sup>

$$\Delta G_{CET} = F(E_{ox} - E_{red}) - E_T + C \quad (10)$$

where  $F$  is the Faraday constant and  $E_{red}$  is the reduction potential of molecular oxygen ( $-0.78$  V vs SCE in acetonitrile).<sup>41</sup> The electrostatic interaction energy  $C$  has been neglected in all previous studies and in the present because all data were



determined in the same solvent.<sup>16–18</sup> These studies revealed that empirical linear relationships of the form of eq 11 can be used to describe the dependence of  $k_{CT}^P/m$  on  $\Delta G_{CET}$

$$\log(k_{CT}^P/m) = \log(c^P/m) + c_1 - c_2 \Delta G_{CET} \quad (11)$$

$c_1$  and  $c_2$  are positive empirical constants which are characteristic for each series.<sup>16–18</sup> Three studies clearly established that different correlations exist for each  $O_2$  product state, which means that the three channels have a different statistical weight. This is expressed by the constant  $c^P$  in eq 11, which was determined to be  $c^{1\Sigma} = 0.67$ ,  $c^{1\Delta} = 0.33$ , and  $c^{3\Sigma} = 3.00$ , for formation of  $O_2(^1\Sigma_g^+)$ ,  $O_2(^1\Delta_g)$ , and  $O_2(^3\Sigma_g^-)$ , respectively.<sup>16–18</sup> These weight factors imply that the graduation  $k_{CT}^{3\Sigma}/3 > k_{CT}^{1\Sigma} > k_{CT}^{1\Delta}$  holds true. Thus, the charge-transfer induced formation of singlet oxygen is not governed by an energy gap law, because in this case the graduation  $k_{CT}^{1\Sigma} > k_{CT}^{1\Delta} > k_{CT}^{3\Sigma}/3$  would result.<sup>16–18</sup> Therefore, the decay of excited pCT exciplexes to lower-lying pCT complexes (labeled  $k_{ic}^{1\Sigma}$ ,  $k_{ic}^{1\Delta}$ , and  $k_{ic}^{3\Sigma}$  in Figure 1) cannot be rate determining. This was unexpected, because previous temperature-dependent measurements of McLean and Rodgers<sup>29,42,43</sup> showed that  $O_2$  quenching of several triplet states is associated with slightly negative activation enthalpies ( $\Delta H^\ddagger$ ) of about  $-5 \text{ kJ mol}^{-1}$  in the high temperature region, a behavior which these authors explained by the formation of a preequilibrium at the level of the exciplex, which would mean that exciplex decay has to be rate determining. However, later studies of Rau et al. showed that negative activation enthalpies do not necessarily imply preequilibrium conditions.<sup>44,45</sup> The position of the transition state on the hypersurface of the reaction coordinate is defined by the maximum of the activation free energy  $\Delta G^\ddagger$ . At this point of the reaction coordinate,  $\Delta H^\ddagger = \Delta G^\ddagger + T\Delta S^\ddagger$  can be negative, if the corresponding activation entropy  $\Delta S^\ddagger$  is negative enough. Thus, an elementary reaction may exhibit a negative enthalpy of activation too. This has been demonstrated by Rau et al. for photoinduced electron transfer from excited [tris(2,2'-bipyridine)ruthenium(II)]<sup>2+</sup> to some anthraquinones with small positive or negative Gibbs energies of reaction.<sup>45</sup> Thus, the formation of  $^1,3(T_1^3\Sigma)$  exciplexes from  $^1,3(T_1^3\Sigma)$  encounter complexes could well be rate-determining. Finally, the unexpected graduation of rate constants reported for the pCT channel in several papers also implies that there is no isc at the level of the pCT complexes, because isc would establish an energy-gap dependent behavior.<sup>16–18</sup> This was also unexpected, because, in the absence of experimental evidence, all previous investigations assumed that isc takes place at the level of both nCT encounter complexes and pCT exciplexes.<sup>11–13,31</sup>

Mehrdad et al.<sup>18</sup> explained this behavior by a mechanism where isc in the nCT complexes is coupled to the rotation of the  $O_2$  molecule (which is estimated to be significantly faster than the decay of nCT complexes), whereas in the pCT complexes, rotation (and thus isc) is restricted by significant noncovalent binding of the  $O_2$  molecule to the aromatic ring of a  $\pi\pi^*$  sensitizer. This is also in agreement with the previously suggested oriented supra–supra structure of the pCT complexes,<sup>19–21</sup> which is thought to be similar to that formed during pCT induced deactivation of  $O_2(^1\Delta_g)$  by benzene.<sup>46</sup> The limiting structures of nCT and pCT complexes are also represented in Figure 1.

Additionally, information on the energetics of structural changes associated with the charge-transfer process have been obtained from a Marcus-type interpretation of experimental data, from which reorganization energies ( $\lambda$ ) can be calculated.<sup>47</sup> These can be separated into an intramolecular contribution ( $\lambda_i$ )

and a solvent dependent part ( $\lambda_o$ ), if the amount of charge transferred (i.e.,  $\delta$ ) is known.<sup>48</sup> Estimates of  $\delta$  according to a Marcus-type model led to  $\lambda_i$  values of the order of  $30 \text{ kJ mol}^{-1}$  for a series of naphthalene and biphenyl derivatives and to a strong increase of  $\lambda_o$  with increasing solvent polarity, from  $1.4 \text{ kJ mol}^{-1}$  ( $CCl_4$ ) to  $60 \text{ kJ mol}^{-1}$  ( $CH_3CN$ ).<sup>20</sup>

Finally, it is important to know that all mechanistic conclusions described here apply exclusively to  $\pi\pi^*$  excited triplets. Although the very vast majority of singlet oxygen sensitizers have a  $\pi\pi^*$  triplet state configuration, it should be noted that  $n\pi^*$  excited ketones exhibit a significantly different behavior, which has been previously discussed in detail.<sup>21,49</sup>

Hence, the mechanism of singlet oxygen photosensitization during  $O_2$  quenching of triplet states seems to be well-established. However, two important points remained unclear in previous work: First, the  $E_{ox}$  values of the compounds studied in ref 34 were unknown, and hence, the influence of CT interactions could not be quantitatively understood in this investigation. Additionally, recent work has raised the question, to what extent  $k_{\Delta E}^P/m$  is influenced by the molecular structure of the sensitizer.<sup>18</sup> To address these two issues, and to find out whether *one* dependence on  $\Delta E$  and  $\Delta G_{CET}$  describes the values of  $k_T^P/m$  in a general way and whether the mechanism described here can be generally applied to  $\pi\pi^*$  excited triplets, we have now extended our study to a series of compounds with strongly varying molecular structure and determined the  $E_{ox}$  values of all previously investigated sensitizers.

## Experimental Section

Carbon tetrachloride (Acros, 99+%,  $Al_2O_3$ ) and phenalene (Aldrich, 97%,  $CH_2Cl_2$ /silica gel) were purified by column chromatography. Quinoxaline (Aldrich, 99%) was vacuum sublimed. Water-free acetonitrile (Merck, Selectipur), coumarin (ICN Biomedicals), chrysene (Aldrich, 95%), benzo[*h*]quinoline (Aldrich, 97%), pyrene-1-carboxaldehyde (Lancaster, 99%), dibenzo[*a,c*]anthracene (Aldrich, 97%), tetrachloro-*p*-benzoquinone (Janssen Chimica, 99%), tetraphenylporphine zinc (Aldrich), octaethylporphine zinc (Aldrich, 98%), fullerene  $C_{60}$  (Lancaster, 99+%), fullerene  $C_{70}$  (Lancaster, 98%), tetraphenylporphine (Aldrich, 99%), phenazine (Aldrich, 98%), acridine (Aldrich, 97%), benzanthrone (Lancaster, 99+%), fluorenone (Aldrich, 98%), 2-acetonaphthone (Aldrich, 99%), 4-benzoyl-biphenyl (Aldrich, 99%), triphenylene (Aldrich, 98%), and tetrabutylammoniumhexafluorophosphate (Aldrich, 98%) were used as received. Solutions for luminescence measurements were prepared and filled into sample cells in a glovebox under dry atmosphere to avoid the uptake of humidity in the investigation of  $O_2(^1\Sigma_g^+)$ . Irradiation was provided by a XeCl excimer laser (ATL Lasertechnik) at 308 nm. The  $O_2(^1\Sigma_g^+ \rightarrow ^3\Sigma_g^-)$  phosphorescence was recorded at 764 nm using a Hamamatsu PM R1464 photomultiplier, the  $O_2(^1\Sigma_g^+ \rightarrow ^1\Delta_g)$  fluorescence was detected at 1940 nm using a liquid  $N_2$ -cooled InAs diode (EG&G Judson J12-D) with a preamplifier (EG&G Judson PA7), and the  $O_2(^1\Delta_g \rightarrow ^3\Sigma_g^-)$  phosphorescence was recorded at 1275 nm using a cryogenic Ge diode (North Coast EO817P). Luminescence signals were digitized using a digital storage oscilloscope (Tektronix TDS210 or TDS3052). All signals were recorded at room temperature, in air-saturated solutions of dry  $CCl_4$ , in the absence and presence of 7 vol % benzene. The method used for the determination of the rate constants  $k_T^{1\Sigma}$ ,  $k_T^{1\Delta}$ , and  $k_T^{3\Sigma}$  of formation of  $O_2(^1\Sigma_g^+)$ ,  $O_2(^1\Delta_g)$ , and  $O_2(^3\Sigma_g^-)$  has been previously described in detail.<sup>1,33</sup> All sensitizers were directly irradiated at 308 nm. A total of 16 laser shots were averaged for  $O_2(^1\Sigma_g^+ \rightarrow ^1\Delta_g)$  and  $O_2(^1\Delta_g \rightarrow ^3\Sigma_g^-)$  signals and

**TABLE 1: Ionization Energies IE and Measured and Estimated Oxidation Potentials  $E_{\text{ox}}^n$** 

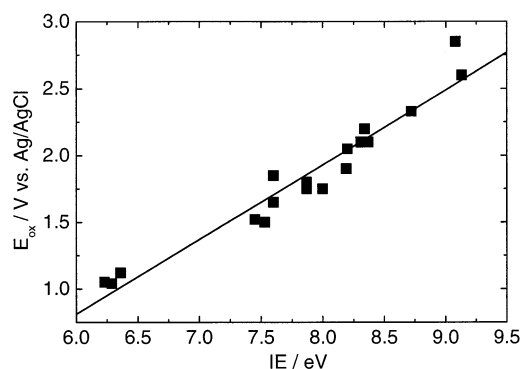
| compound                            | IE,<br>eV           | $E_{\text{ox}},$<br>V vs Ag/AgCl | $E_{\text{ox}},$<br>V vs SCE |
|-------------------------------------|---------------------|----------------------------------|------------------------------|
| octaethylporphine zinc              | 6.29 <sup>a</sup>   | 1.04                             | 0.95 <sup>g</sup>            |
| tetraphenylporphine zinc            | 6.23 <sup>a</sup>   | 1.05 <sup>l</sup>                | 0.96 <sup>h</sup>            |
| tetraphenylporphine                 | 6.36 <sup>a</sup>   | 1.12 <sup>l</sup>                | 1.03 <sup>l</sup>            |
| 9-bromoanthracene                   | 7.53 <sup>a,c</sup> | 1.50                             | 1.41                         |
| dibenzo[ <i>a,h</i> ]anthracene     | 7.45 <sup>a,b</sup> | 1.52                             | 1.43                         |
| pyrene-1-carboxyaldehyde            |                     | 1.54                             | 1.45                         |
| chrysene                            | 7.60 <sup>d</sup>   | 1.65                             | 1.56                         |
| acridine                            | 7.87 <sup>a,b</sup> | 1.75                             | 1.66                         |
| benzanthrone                        | 8.00 <sup>e</sup>   | 1.75                             | 1.66                         |
| triphenylene                        | 7.87 <sup>d</sup>   | 1.80                             | 1.71                         |
| fullerene C <sub>60</sub>           | 7.60 <sup>f</sup>   | 1.85 <sup>l</sup>                | 1.76 <sup>l</sup>            |
| fullerene C <sub>70</sub>           | 7.60 <sup>f</sup>   | 1.85 <sup>l</sup>                | 1.76 <sup>l</sup>            |
| benzo[ <i>h</i> ]quinoline          | 8.19 <sup>a,b</sup> | 1.90                             | 1.81                         |
| phenalene                           | 8.20 <sup>a</sup>   | 2.05                             | 1.96                         |
| 2-acetonaphthone                    | 8.31 <sup>a</sup>   | 2.10                             | 2.01                         |
| phenazine                           | 8.37 <sup>a</sup>   | 2.10                             | 2.01                         |
| fluorenone                          | 8.34                | 2.20                             | 2.11                         |
| 4-benzoylbiphenyl                   |                     | 2.22                             | 2.13                         |
| coumarin                            | 8.72 <sup>e</sup>   | 2.33                             | 2.24                         |
| quinoxaline                         | 9.01 <sup>d</sup>   | 2.50 <sup>m</sup>                | 2.41                         |
| duroquinone                         | 9.17 <sup>a</sup>   | 2.59 <sup>m</sup>                | 2.50                         |
| 4-methylbenzophenone                | 9.13 <sup>b</sup>   | 2.60 <sup>k</sup>                | 2.51                         |
| benzophenone                        | 9.08 <sup>d</sup>   | 2.85 <sup>k</sup>                | 2.76                         |
| tetrachloro- <i>p</i> -benzoquinone | 9.82 <sup>a</sup>   | 2.95 <sup>m</sup>                | 2.86                         |

<sup>a</sup> Reference 54. <sup>b</sup> Reference 55. <sup>c</sup> Reference 56. <sup>d</sup> Reference 57. <sup>e</sup> Reference 58. <sup>f</sup> Reference 59. <sup>g</sup> Reference 60. <sup>h</sup> Reference 61. <sup>i</sup> Reference 62. <sup>j</sup> Reference 63. <sup>k</sup> Reference 21. <sup>l</sup> Measured vs SCE. <sup>m</sup> Estimated by the correlation  $E_{\text{ox}} = 0.5602 \text{ IE} - 2.55$ . <sup>n</sup> All  $E_{\text{ox}}$  values have been measured vs Ag/AgCl reference electrode unless otherwise noted. SCE values are obtained by subtracting 0.09 V from values measured vs Ag/AgCl.

at least 64 shots for  $\text{O}_2(^1\Sigma_g^+ \rightarrow ^3\Sigma_g^-)$  signals. Only energy-independent results are reported.

The values of  $E_{\text{ox}}$  listed in Table 1 were determined by cyclic voltammetry. They are interpreted as one-electron oxidations of the neutral organic molecules to the corresponding radical cations. This is supported by the peak currents of the oxidation waves being nearly equal to that of a reversible one-electron oxidation (e.g., of perylene) at the same concentration. The cyclic voltammograms were not reversible, because the reverse reduction peaks were found to be diminished or even absent. If a reverse peak was observed, e.g., for 2,7-dibromofluorene,<sup>18</sup> the separation of oxidation and reduction peaks amounted about 60 mV. It is assumed that the reversible one-electron transfer is followed by some irreversible chemical reaction of the radical cations. In such a so-called  $E_rC_i$  system (reversible electron transfer with consecutive irreversible chemical reaction), the peak potential depends on the rate constant  $k$  of the follow-up reaction shifting it to more negative values by about 30 mV per 10-fold increase of  $k$  with respect to the peak potential of a pure  $E_r$  system. Thus, accurate redox potentials cannot be evaluated. However, assuming that the variation of  $k$  does not exceed 3 orders of magnitude in the different systems with respect to the reversible  $E_r$  case at the voltage scan rates used, the  $E_{\text{ox}}$  values reported are considered as lower limits of the thermodynamic redox potentials with an uncertainty of 0.1 V. These values serve as means for the estimation of the extent of charge-transfer interactions in the triplet state quenching by  $\text{O}_2$ .

The cyclic voltammograms were obtained using the Bank POS 73 potentiostat. A three-electrode system was employed with a platinum disk as the working electrode, an Ag/AgCl reference electrode, and a platinum wire as the counter electrode. All measurements were carried out at room temperature, in deoxygenated solutions of water-free acetonitrile containing  $10^{-3}$

**Figure 2.** Correlation of  $E_{\text{ox}}$  vs IE. Data of Table 1. Solid line is given by  $E_{\text{ox}} = 0.5602 \text{ IE} - 2.55$ .**TABLE 2: Experimental Photophysical and Electrochemical Parameters for  $\text{O}_2$  Quenching of  $T_1$  States in  $\text{CCl}_4$** 

| sensitizer                          | $T_1$ yield       | $k_T^Q,$<br>$10^9 \text{ M}^{-1} \text{ s}^{-1c}$ | $S_\Delta^c$ | $a^c$ |
|-------------------------------------|-------------------|---|--------------|-------|
| tetraphenylporphine zinc            | 0.88 <sup>a</sup> | 0.871   | 0.55         |       |
| octaethylporphine zinc              | 1.00 <sup>b</sup> | 1.98  | 0.40         | 0.39  |
| 1-pyrenecarboxyaldehyde             | 0.78 <sup>a</sup> | 1.71  | 0.90         | 0.70  |
| chrysene                            | 0.85 <sup>a</sup> | 1.35  | 0.60         | 0.31  |
| C <sub>60</sub>                     | 1.00 <sup>a</sup> | 1.43  | 0.74         |       |
| C <sub>70</sub>                     | 0.97 <sup>a</sup> | 0.793   | 0.65         |       |
| benzo[ <i>h</i> ]quinoline          | 0.88 <sup>a</sup> | 1.40  | 0.60         | 0.48  |
| quinoxaline                         | 0.99 <sup>a</sup> | 0.65  | 0.95         | 0.88  |
| tetrachloro- <i>p</i> -benzoquinone | 0.98 <sup>a</sup> | 1.32  | 0.91         | 0.74  |

<sup>a</sup> Reference 64. <sup>b</sup> Determined by photoacoustic calorimetry,  $\pm 3\%$ . <sup>c</sup>  $\pm 10\%$ .

M of the sensitizer and 0.1 M tetrabutylammoniumhexafluorophosphate as supporting electrolyte. The voltage scan was varied between 20 and 200  $\text{mV s}^{-1}$ . The data listed refer to the scan rate of 50  $\text{mV s}^{-1}$  throughout.

## Results and Discussion

All newly determined oxidation potentials are listed in Table 1, together with the corresponding gas-phase ionization energies IE.

No peaks were observed with three compounds used in this study, namely, quinoxaline, duroquinone, and tetrachloro-*p*-benzoquinone. A correlation between  $E_{\text{ox}}$  values and gas-phase ionization energies IE is used to estimate their oxidation potentials (see Figure 2, estimated values are listed in Table 1). All IE data have been taken from <http://webbook.nist.gov>. We use "evaluated IE" values, when such values are given, and mean values of all listed IE determinations in all other cases. We will consider below experimental data for a series of naphthalene and biphenyl derivatives, for which all  $E_{\text{ox}}$  data have been measured by Abdel-Shafi and Wilkinson,<sup>11,16</sup> using a SCE reference electrode, in deoxygenated acetonitrile solutions containing  $10^{-3}$  M of the respective derivative, and 0.1 M tetrabutylammonium perchlorate as supporting electrolyte. We have previously noted a systematic shift of 0.09 V between these data and our values measured with tetrabutylammoniumhexafluorophosphate vs Ag/AgCl reference electrode.<sup>21</sup> All new data are converted accordingly, and SCE values are used for calculations of  $\Delta G_{\text{CET}}$ , according to eq 10, where  $C$  is neglected.

Newly determined photophysical data for a series of sensitizers with strongly varying  $E_{\text{ox}}$ ,  $E_T$  and molecular structure are listed in Table 2. These data can be used to calculate the rate constants of formation of  $\text{O}_2(^1\Sigma_g^+)$ ,  $\text{O}_2(^1\Delta_g)$ , and  $\text{O}_2(^3\Sigma_g^-)$ , according to eqs 1–4. All calculated  $k_T^P$  values are listed in Table 3, together with the respective data for all previously

**TABLE 3: Rate Constants  $k_T^{1\Sigma_g^+}$ ,  $k_T^{1\Delta_g}$ , and  $k_T^{3\Sigma_g^-}$  of Formation of  $O_2(^1\Sigma_g^+)$ ,  $O_2(^1\Delta_g)$ , and  $O_2(^3\Sigma_g^-)$  during  $O_2$  Quenching of Triplet Excited Sensitizers and the Corresponding Triplet Energies  $E_T$  and Free Energies  $\Delta G_{CET}$  for a Complete Electron Transfer**

| sensitizer                           | $E_T$                | $\Delta G_{CET}$     | $k_T^{1\Sigma}$       | $k_T^{1\Delta}$       | $k_T^{3\Sigma}$       |
|--------------------------------------|----------------------|----------------------|-----------------------|-----------------------|-----------------------|
|                                      | $\text{kJ mol}^{-1}$ | $\text{kJ mol}^{-1}$ | $10^9 \text{ s}^{-1}$ | $10^9 \text{ s}^{-1}$ | $10^9 \text{ s}^{-1}$ |
| tetraphenylporphine zinc             | 153 <sup>a</sup>     | 15                   |                       | 0.49                  | 0.40                  |
| octaethylporphine zinc               | 170 <sup>a</sup>     | -3                   | 0.83                  |                       | 1.28                  |
| 1-pyrenecarboxaldehyde               | 180 <sup>a</sup>     | 35                   | 1.28                  | 0.36                  | 0.18                  |
| chrysene                             | 239 <sup>a</sup>     | -13                  | 0.44                  | 0.41                  | 0.57                  |
| C <sub>60</sub>                      | 148 <sup>b</sup>     | 88                   |                       | 1.12                  | 0.39                  |
| C <sub>70</sub>                      | 131 <sup>b</sup>     | 105                  |                       | 0.53                  | 0.29                  |
| benzo[h]quinoline                    | 260 <sup>a</sup>     | -10                  | 0.71                  | 0.18                  | 0.59                  |
| quinoxaline                          | 255 <sup>a</sup>     | 50                   | 0.59                  | 0.05                  | 0.03                  |
| tetrachloro- <i>p</i> -benzoquinone  | 206 <sup>a</sup>     | 144                  | 1.03                  | 0.24                  | 0.12                  |
| tetraphenylporphine <sup>c</sup>     | 140                  | 35 <sup>d</sup>      |                       | 1.12                  | 0.41                  |
| 9-bromanthracene <sup>c</sup>        | 168                  | 43 <sup>d</sup>      | 1.32                  | 1.51                  | 0.31                  |
| phenalenone <sup>c</sup>             | 186                  | 78 <sup>d</sup>      | 1.44                  | 0.89                  | 0.07                  |
| phenazine <sup>c</sup>               | 186                  | 83 <sup>d</sup>      | 1.38                  | 0.44                  | 0.08                  |
| acridine <sup>c</sup>                | 189                  | 46 <sup>d</sup>      | 1.44                  | 0.66                  |                       |
| benzanthrone <sup>c</sup>            | 205                  | 30 <sup>d</sup>      | 1.60                  | 0.28                  |                       |
| 9-fluorenone <sup>c</sup>            | 223                  | 56 <sup>d</sup>      | 1.75                  | 0.14                  | 0.06                  |
| duroquinone <sup>c</sup>             | 235                  | 82 <sup>d</sup>      | 1.18                  | 0.37                  | 0.12                  |
| 2-acetonaphthone <sup>c</sup>        | 248                  | 21 <sup>d</sup>      | 1.01                  | 0.21                  | 0.18                  |
| 4-benzoylbiphenyl <sup>c</sup>       | 254                  | 27 <sup>d</sup>      | 0.53                  | 0.05                  | 0.10                  |
| triphenylene <sup>c</sup>            | 278                  | -38 <sup>d</sup>     | 0.30                  |                       | 0.73                  |
| 1-methoxynaphthalene <sup>c</sup>    | 256                  | -59                  | 1.80                  | 0.49                  | 2.10                  |
| acenaphthene <sup>c</sup>            | 250                  | -46                  | 1.51                  | 0.36                  | 1.30                  |
| 2-methoxynaphthalene <sup>c</sup>    | 253                  | -45                  | 1.63                  | 0.29                  | 0.64                  |
| 2,6-dimethylnaphthalene <sup>c</sup> | 252                  | -33                  | 1.59                  | 0.16                  | 0.45                  |
| 1-methylnaphthalene <sup>c</sup>     | 257                  | -33                  | 1.28                  | 0.19                  | 0.35                  |
| 2-methylnaphthalene <sup>c</sup>     | 253                  | -22                  | 1.31                  | 0.18                  | 0.27                  |
| naphthalene <sup>c</sup>             | 255                  | -21                  | 1.12                  | 0.11                  | 0.17                  |
| 1-bromonaphthalene <sup>c</sup>      | 247                  | -1                   | 1.10                  | 0.11                  | 0.02                  |
| 1-cyanonaphthalene <sup>c</sup>      | 243                  | 26                   | 0.81                  | 0.12                  | 0.02                  |
| 4,4'-dimethoxybiphenyl <sup>f</sup>  | 266                  | -65                  | 4.45                  | 1.86                  | 13.31                 |
| 4-methoxybiphenyl <sup>f</sup>       | 270                  | -47                  | 1.47                  | 0.33                  | 3.14                  |
| 4,4'-dimethylbiphenyl <sup>f</sup>   | 269                  | -31                  | 1.31                  | 0.26                  | 0.95                  |
| 4-methylbiphenyl <sup>f</sup>        | 272                  | -23                  | 0.91                  | 0.18                  | 0.46                  |
| biphenyl <sup>f</sup>                | 274                  | -15                  | 0.61                  | 0.10                  | 0.31                  |
| 4-chlorobiphenyl <sup>f</sup>        | 269                  | -5                   | 0.65                  | 0.10                  | 0.15                  |
| 4-bromobiphenyl <sup>f</sup>         | 266                  | -3                   | 0.64                  | 0.08                  | 0.12                  |
| 4,4'-dibromobiphenyl <sup>f</sup>    | 265                  | 4                    | 0.70                  | 0.05                  | 0.06                  |
| 4,4'-dichlorobiphenyl                | 265                  | 5                    | 0.62                  | 0.09                  | 0.10                  |
| 4-cyanobiphenyl <sup>f</sup>         | 265                  | 14                   | 0.54                  | 0.07                  | 0.05                  |
| 2-methylfluorene <sup>g</sup>        | 282                  | -59                  | 0.68                  | 0.24                  | 1.42                  |
| 1-methylfluorene <sup>g</sup>        | 284                  | -54                  | 0.60                  | 0.31                  | 2.28                  |
| fluorene <sup>g</sup>                | 285                  | -51                  | 0.86                  | 0.42                  | 2.53                  |
| 2-bromofluorene <sup>g</sup>         | 276                  | -36                  | 0.61                  | 0.16                  | 1.04                  |
| 2,7-dibromofluorene <sup>g</sup>     | 270                  | -18                  | 0.47                  | 0.13                  | 0.52                  |
| 2,4,7-trichlorofluorene <sup>g</sup> | 273                  | -9                   | 0.38                  | 0.06                  | 0.22                  |

<sup>a</sup> Reference 64. <sup>b</sup> Reference 65. <sup>c</sup> Reference 34. <sup>d</sup> This work. <sup>e</sup> Reference 16. <sup>f</sup> Reference 17. <sup>g</sup> Reference 18.

investigated sensitizers<sup>16–18</sup> and the corresponding  $\Delta G_{CET}$  and  $E_T$  data.

Figure 3 shows the dependence of all multiplicity-normalized  $k_T^{1\Sigma}$ ,  $k_T^{1\Delta}$ , and  $k_T^{3\Sigma}$  values on  $\Delta E$  and  $\Delta G_{CET}$  and thus on  $E_T$  and  $E_{ox}$ . It is shown that the whole data set, which covers the  $\Delta E$  and  $\Delta G_{CET}$  range of most natural and synthetic sensitizers, and includes aromatic hydrocarbons composed of very variable numbers of five- and/or six-membered rings, with and without heteroatoms, or even metal centers, and bearing many different types of substituents, is described by one surface calculated using eqs 6–8, where the nCT and CT contributions have been estimated by eqs 9 and 11, with  $c_1 = 7.65$  and  $c_2 = 0.023 \text{ kJ mol}^{-1}$ . (For clarity reasons, eq 11 was approximated using  $c^P/m = 1$  for formation of all three  $O_2$  product states. The actual model predicts three distinct but closely lying surfaces, for formation of  $O_2(^1\Sigma_g^+)$ ,  $O_2(^1\Delta_g)$ , and  $O_2(^3\Sigma_g^-)$ , respectively, and describes the data better than represented in Figure 3. Standard deviation of experimental vs calculated data of  $\log(k_T^P/m)$

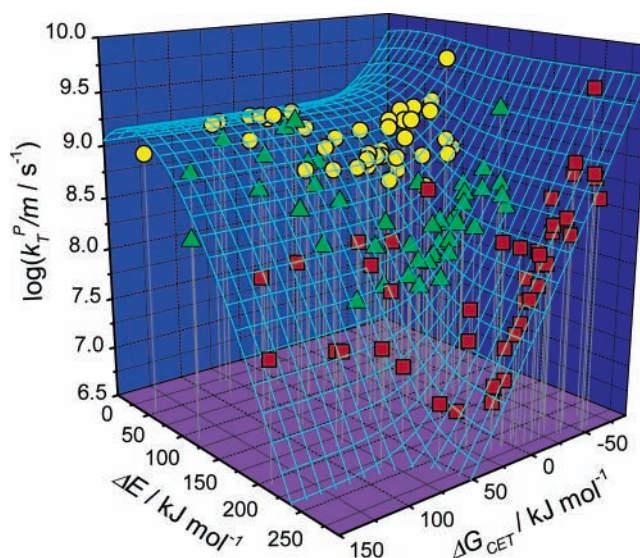


**Figure 3.** Dependence of the multiplicity-normalized rate constants  $k_T^P/m$  of formation of  $O_2(^1\Sigma_g^+)$  (circles),  $O_2(^1\Delta_g)$  (triangles), and  $O_2(^3\Sigma_g^-)$  (squares) during  $O_2$  quenching of  $\pi\pi^*$  triplet states on the excess energy  $\Delta E$  for formation of the respective  $O_2$  product state and the free energy  $\Delta G_{CET}$  for formation of an ion pair. Surface calculated by  $k_T^P/m = k_{\Delta E}^P/m + k_{CT}^P/m$ , using  $\log(k_{\Delta E}^P/m) = 9.05 + 9 \times 10^{-3} \Delta E - 1.15 \times 10^{-4} \Delta E^2 + 1.15 \times 10^{-7} \Delta E^3 + 9.1 \times 10^{-11} \Delta E^4$ , and  $\log(k_{CT}^P/m) = 7.65 - 0.023 \Delta G_{CET}$ .

amounts to 0.27, which corresponds to a factor of 1.8 in  $k_T^P/m$ , which is rather small, if the overall variation of  $k_T^P/m$  by the factor of 750 is considered.)

However, deviations of experimental from calculated data are in part larger than the experimental uncertainties. This is most probably a result of the general neglect of the electrostatic interaction energy  $C$ , which is positive in the nonpolar solvent  $CCl_4$  and which depends on the widely varying molecular structure of the sensitizers. An additional but less important source of uncertainty of the values of  $\Delta G_{CET}$  results from the uncertainty of the  $E_{ox}$  data. Nonetheless, the description of the data by eqs 6–11 is still surprisingly good, and we demonstrate clearly that  $E_T$  and  $E_{ox}$  are by far the most important parameters determining  $k_T^{1\Sigma}$ ,  $k_T^{1\Delta}$ , and  $k_T^{3\Sigma}$ . This also means that the mechanism of singlet oxygen photosensitization via nCT and CT complexes described in Figure 1 can be generally applied to  $\pi\pi^*$  excited triplets. Figure 3 shows that the nCT path dominates for sensitizers with  $\Delta G_{CET} \geq 50 \text{ kJ mol}^{-1}$ , i.e., on the left-hand side. The additional quenching via the pCT channel becomes only important in the exergonic range and dominates for sensitizers with  $\Delta G_{CET} \leq -25 \text{ kJ mol}^{-1}$ , i.e., on the right border of the calculated surface.

The general validity of the model also shows that eqs 6–11 can be used to estimate the rate constants and efficiencies of singlet oxygen formation during  $O_2$  quenching of  $T_1$  states of  $\pi\pi^*$  excited aromatic hydrocarbons as a function of sensitizer  $E_{ox}$  and  $E_T$ . The rate constants of formation of  $O_2(^1\Sigma_g^+)$ ,  $O_2(^1\Delta_g)$ , and  $O_2(^3\Sigma_g^-)$  can be simply calculated from eqs 6–11, and since deactivation of  $O_2(^1\Sigma_g^+)$  to  $O_2(^1\Delta_g)$  is a quantitative process, the overall efficiency  $S_\Delta$  of singlet oxygen formation, which is the relevant parameter in most applications, can be calculated by eq 12

$$S_\Delta = \frac{k_T^{1\Sigma} + k_T^{1\Delta}}{k_T^{1\Sigma} + k_T^{1\Delta} + k_T^{3\Sigma}} \quad (12)$$

Because of the extremely short lifetime of  $O_2(^1\Sigma_g^+)$  in most



solvents,<sup>2</sup> the measurements described in this work have so far only been possible in solutions of CCl<sub>4</sub>, and thus, the direct application of our results is only valid in this solvent. However, it is well-established that medium-dependent variations of  $k_T^Q$  and  $S_\Delta$  exhibit a systematic dependence on solvent polarity. It has been reported that  $k_T^Q$  for several series of sensitizers increases significantly with increasing solvent polarity, while  $S_\Delta$  decreases.<sup>8,9,12,15,19–21,31</sup> Hence, the present model can be used to estimate relative values in other media. Although other parameters, such as sensitizer aggregation (which was generally found to diminish the singlet oxygen yield of a sensitizer)<sup>50–53</sup> might come into play in several media, and especially in biological situations, it is believed that the relations presented here will be most useful for the optimization of the inherent properties of molecules with regard to their singlet oxygen photosensitization ability and, thus, also for the development of efficient singlet oxygen sensitizers for several applications. One important restriction, however, needs to be made: The correlation does not apply to  $n\pi^*$  excited triplets, where a different quenching mechanism operates.<sup>21,49</sup>

**Acknowledgment.** Financial support by the Deutsche Forschungsgemeinschaft and the Adolf Messer Stiftung is greatly appreciated. C.S. thanks the Ministère de la Culture, de l'Enseignement Supérieur et de la Recherche of Luxembourg for a BFR scholarship.

## References and Notes

- Schmidt, R.; Bodesheim, M. *Chem. Phys. Lett.* **1993**, *213*, 111.
- Schmidt, R.; Bodesheim, M. *J. Phys. Chem. A* **1998**, *102*, 4769.
- Gijzeman, O. L. J.; Kaufman, F.; Porter, G. *J. Chem. Soc., Faraday Trans. 2* **1973**, *69*, 708.
- Wilkinson, F.; Helman, W. P.; Ross, A. B. *J. Phys. Chem. Ref. Data* **1993**, *22*, 113.
- Redmond, R. W.; Gamlin, J. N. *Photochem. Photobiol.* **1999**, *70*, 391.
- Garner, A.; Wilkinson, F. *Chem. Phys. Lett.* **1977**, *45*, 432.
- McGarvey, D. J.; Szekeres, P. G.; Wilkinson, F. *Chem. Phys. Lett.* **1992**, *199*, 314.
- Wilkinson, F.; McGarvey, D. J.; Olea, A. F. *J. Am. Chem. Soc.* **1993**, *115*, 12144.
- Wilkinson, F.; McGarvey, D. J.; Olea, A. F. *J. Phys. Chem.* **1994**, *98*, 3762.
- Olea, A. F.; Wilkinson, F. *J. Phys. Chem.* **1995**, *99*, 4518.
- Wilkinson, F.; Abdel-Shafi, A. A. *J. Phys. Chem. A* **1997**, *101*, 5509.
- Wilkinson, F.; Abdel-Shafi, A. A. *J. Phys. Chem. A* **1999**, *103*, 5425.
- Abdel-Shafi, A. A.; Wilkinson, F. *J. Phys. Chem. A* **2000**, *104*, 5747.
- Abdel-Shafi, A. A.; Worrall, D. R.; Wilkinson, F. *Photochem. Photobiol. A: Chem.* **2001**, *142*, 133.
- Abdel-Shafi, A. A.; Wilkinson, F. *Phys. Chem. Chem. Phys.* **2002**, *4*, 248.
- Schmidt, R.; Shafii, F.; Schweitzer, C.; Abdel-Shafi, A. A.; Wilkinson, F. *J. Phys. Chem. A* **2001**, *105*, 1811.
- Schmidt, R.; Shafii, F. *J. Phys. Chem. A* **2001**, *105*, 8871.
- Mehrdad, Z.; Noll, A.; Grabner, E.-W.; Schmidt, R. *Photochem. Photobiol. Sci.* **2002**, *1*, 263.
- Schweitzer, C.; Mehrdad, Z.; Shafii, F.; Schmidt, R. *J. Phys. Chem. A* **2001**, *105*, 5309.
- Schweitzer, C.; Mehrdad, Z.; Shafii, F.; Schmidt, R. *Phys. Chem. Chem. Phys.* **2001**, *3*, 3095.
- Schweitzer, C.; Mehrdad, Z.; Noll, A.; Grabner, E.-W.; Schmidt, R. *Helv. Chim. Acta* **2001**, *84*, 2493.
- Demas, J. N.; Harris, E. W.; McBride, R. P. *J. Am. Chem. Soc.* **1977**, *99*, 3547.
- Cebul, F. A.; Kirk, K. A.; Lupo, D. W.; Pittenger, L. M.; Schuh, M. D.; Williams, I. F.; Winston, G. C. *J. Am. Chem. Soc.* **1980**, *102*, 5656.
- Wilson, T.; Halpern, A. M. *J. Am. Chem. Soc.* **1980**, *102*, 7279.
- Levin, P. P.; Pluzhnikov, P. F.; Kuzmin, V. A. *Chem. Phys. Lett.* **1988**, *152*, 409.
- Yasuda, H.; Scully, A. D.; Hirayama, S.; Okamoto, M.; Tanaka, F. *J. Am. Chem. Soc.* **1990**, *112*, 6847.
- Okamoto, M.; Tanaka, F. *J. Phys. Chem. A* **2002**, *106*, 3982.
- Grewer, C.; Brauer, H.-D. *J. Phys. Chem.* **1993**, *97*, 5001.
- McLean, A. J.; Rodgers, M. A. J. *J. Am. Chem. Soc.* **1993**, *115*, 9874.
- Hirayama, S.; Yasuda, H.; Scully, A. D.; Okamoto, M. *J. Phys. Chem.* **1994**, *98*, 4609.
- Darmanyan, A. P.; Lee, W.; Jenks, W. S. *J. Phys. Chem. A* **1999**, *103*, 2705.
- Grewer, C.; Brauer, H.-D. *J. Phys. Chem.* **1994**, *98*, 4230.
- Shafii, F.; Schmidt, R. *J. Phys. Chem. A* **2001**, *105*, 1805.
- Bodesheim, M.; Schütz, M.; Schmidt, R. *Chem. Phys. Lett.* **1994**, *221*, 7.
- Kawaoka, K.; Khan, A. U.; Kearns, D. R. *J. Chem. Phys.* **1967**, *46*, 1842.
- Siebrand, W.; Williams, D. F. *J. Chem. Phys.* **1967**, *46*, 403.
- Siebrand, W. *J. Chem. Phys.* **1967**, *47*, 2411.
- Siebrand, W.; Williams, D. F. *J. Chem. Phys.* **1968**, *49*, 1860.
- Rehm, D.; Weller, A. *Isr. J. Chem.* **1970**, *8*, 259.
- Weller, A. *Z. Phys. Chem. Neue Folge* **1982**, *133*, 93.
- Mattes, S. L.; Farid, S. In *Organic Photochemistry*; Padwa, A., Ed.; Marcel Dekker: New York, 1983.
- McLean, A. J.; Rodgers, M. A. J. *J. Am. Chem. Soc.* **1992**, *114*, 3145.
- McLean, A. J.; Rodgers, M. A. J. *J. Am. Chem. Soc.* **1993**, *115*, 4786.
- Kapinus, E. I.; Rau, H. *J. Phys. Chem. A* **1998**, *102*, 5569.
- Frank, R.; Greiner, G.; Rau, H. *Phys. Chem. Chem. Phys.* **1999**, *1*, 3481.
- Bobrowski, M.; Liwo, A.; Oldziej, S.; Jeziorek, D.; Ossowski, T. *J. Am. Chem. Soc.* **2000**, *122*, 8112.
- Marcus, R. A. *Annu. Rev. Phys. Chem.* **1964**, *15*, 155.
- Sutin, N. *Prog. Inorg. Chem.* **1983**, *30*, 441.
- Mehrdad, Z.; Schweitzer, C.; Schmidt, R. *J. Phys. Chem. A* **2002**, *106*, 228.
- Tanielian, C.; Heinrich, G. *Photochem. Photobiol.* **1995**, *61*, 131.
- Tanielian, C.; Wolff, C.; Esch, M. *J. Phys. Chem.* **1996**, *100*, 6555.
- Tanielian, C.; Schweitzer, C.; Mechin, R.; Wolff, C. *Free Radic. Biol. Med.* **2001**, *30*, 208.
- Dairou, J.; Vever-Bizet, C.; Brault, D. *Photochem. Photobiol.* **2002**, *75*, 229.
- Lias, S. G.; Levin, R. D.; Kafafi, S. A. *Ion Energetics Data in NIST Chemistry WebBook, NIST Standard Reference Database Number 69*; Mallard, W. G., Linstrom, P. J., Eds.; National Institute of Standards and Technology: Gaithersburg, MD, 2000.
- Rosenstock, H. M.; Draxl, K.; Steiner, B. W.; Herron, J. T. *Ion Energetics Data in NIST Chemistry WebBook, NIST Standard Reference Database Number 69*; Mallard, W. G., Linstrom, P. J., Eds.; National Institute of Standards and Technology: Gaithersburg, MD, 2000.
- Lias, S. G.; Bartmess, J. E.; Liebman, J. F.; Holmes, J. L.; Levin, R. D.; Mallard, W. G. *Ion Energetics Data in NIST Chemistry WebBook, NIST Standard Reference Database Number 69*; Mallard, W. G., Linstrom, P. J., Eds.; National Institute of Standards and Technology: Gaithersburg, MD, 2000.
- Lias, S. G. *Ion Energetics Data in NIST Chemistry WebBook, NIST Standard Reference Database Number 69*; Mallard, W. G.; Linstrom, P. J., Eds.; National Institute of Standards and Technology: Gaithersburg, MD, 2000.
- Lias, S. G.; Liebman, J. F. *Ion Energetics Data in NIST Chemistry WebBook, NIST Standard Reference Database Number 69*; Mallard, W. G., Linstrom, P. J., Eds.; National Institute of Standards and Technology: Gaithersburg, MD, 2000.
- Echegoyen, L.; Echegoyen, L. E. *Acc. Chem. Res.* **1998**, *31*, 593.
- Leung, H.-K.; Zhang, G.-Z.; Gan, W.-X.; Chan, Y.-Y. *J. Chem. Soc., Chem. Commun.* **1987**, 20.
- Hinman, A. S.; Pons, S.; Cassidy, J. *Electrochim. Acta* **1985**, *30*, 95.
- Kadish, K. M.; Morrison, M. M. *J. Am. Chem. Soc.* **1976**, *98*, 3326.
- Dubois, D.; Kadish, K. M.; Flanagan, S.; Wilson, L. J. *J. Am. Chem. Soc.* **1991**, *113*, 7773.
- Murov, S. L.; Carmichael, I.; Hug, G. L. *Handbook of Photochemistry*; Marcel Dekker: New York, 1993.
- Dunsbach, R. PhD Thesis, Universität Frankfurt, Frankfurt, Germany, 1993.